XIV International Conference on Computational Plasticity. Fundamentals and Applications
COMPLAS XIV
E. Oñate, D.R.J. Owen, D. Peric & M. Chiumenti (Eds)

3D MODELING OF THE VANE TEST ON A POWER-LAW CEMENT PASTE BY MEANS OF THE PROPER GENERALIZED DECOMPOSITION

CHADY GHNATIOS* AND GERARD-PHILIPPE ZEHIL†

* Notre Dame University - Louaizé
Department of Mechanical Engineering
Zouk Mosbeh, P.O. Box 72, Lebanon
e-mail: cghnatios@ndu.edu.lb

†Notre Dame University - Louaizé
Department of Civil & Environmental Engineering
Zouk Mosbeh, P.O. Box 72, Lebanon
e-mail: gpzehil@ndu.edu.lb

Key words: Cement paste, Vane test, Proper Generalized Decomposition, Power-law fluid, non-linear model

Abstract. The effective modeling of the flow of fresh concrete materials in settings such as that of the vane test is a challenging process that is the object of ongoing research. Previous works modeled concrete and cement pastes as solids subjected to yielding or as Bingham or power-law fluids, both in two or three dimensions [1, 2]. Of the existing models, those implementing power-law fluids in three dimensions carry the best predictive ability considering the typically heterogeneous composition of concrete suspensions and the relatively complex three-dimensional features of their flows.

In this work, we model the vane test in a power-law cement paste using the Proper Generalized Decomposition (PGD). In this framework, the three-dimensional problem is solved as a sequence of $2D \times 1D$ problems, thus alleviating the curse of dimensionality. This choice is supported by experience from previous works using the PGD to simulate Non-Newtonian behavior using iterative resolutions [3, 4]. It is also particularly useful in addressing the inverse problem corresponding to the identification of the material properties of cement pastes from experimental data, as this requires many direct resolutions of the forward problem. The use of the PGD is also appealing because the model parameters can be introduced as extra coordinates of the problem [5].

1 INTRODUCTION

Cement paste characterization is an active field of research. Many cement paste material models currently exist in the relevant literature, based on different physics. Some

works attempt to model cement pastes as solids subjected to yielding [1] while others rely on Brinkman or Power-law fluids [2]. Both types of models have good predictive abilities, although fluid models accounting for suspended particles – such as Non-Newtonian power-law fluids – have a slight advantage.

The conventional vane test consists of a vane rotating inside of a cylinder containing a fluid that must be characterized. The test determines the properties of liquids by measuring the torque on the vane axis [6]. For example, the vane test is used to measure concrete properties based on solid models in [7]. Vane test measurements can also be used to identify the Non-Newtonian power-law properties of cement pastes.

During the vane tests considered in this work, the mixing velocity is increased gradually, at a rate that is sufficiently slow for steady-state conditions to be assumed at every computational time step. To identify material properties using this test, one may need to solve the system of partial differential equations modeling the forward problem at each iteration of an inverse optimization algorithm. The use of the Proper Generalized Decomposition (PGD) is particularly appealing in this case, since the material parameters as well as the angular mixing velocity can be included as extra coordinates of the problem [8, 9]. The result is therefore a "Computational Vademecum" or a "book of solutions," which can be used on the fly to evaluate the quantities of interest during the optimization process of the inverse algorithm.

The PGD's suitability to tackle multidimensional linear problems using the domain separation process is clearly established, with dramatic computational time reductions [10, 11]. However, to the knowledge of the authors, the PGD is not frequently used to resolve multidimensional nonlinear problems. Some works have tackled space domains separations, without including any extra parameters as coordinates of the problem [12, 4]. A few other works have illustrated the ability to simulate nonlinear thermal models using parameters as extra coordinates by combining the PGD and the Proper Orthogonal Decomposition (POD) [9, 13]. In this work, we use the Proper Generalized Decomposition to simulate Non-Newtonian power-law fluid in a vane test while considering the process parameters as extra-coordinates of the problem.

2 MODELING THE VANE TEST

In this section we describe the modeling of the vane test using Non-Newtonian power-law fluids. The modeled vane test has the dimensions shown in Figure 1. Because the problem is not axisymmetric, a three-dimensional simulation is necessary to capture the fluid flow.

Designating by $\mathbf{v}$ the velocity vector, the conservation of mass in the modeled fluid region can be written as:

$$\nabla \cdot \mathbf{v} = 0. \tag{1}$$

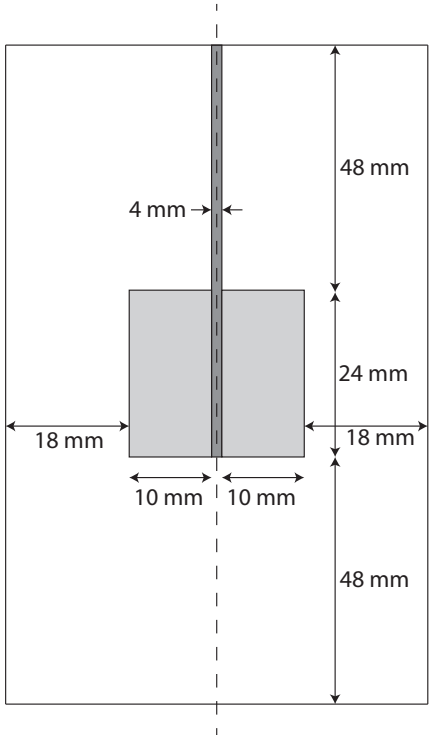

Figure 1: Modeled vane test dimensions.

For the test considered, the angular velocity imposed to the rotating vane changes very slowly. The mixing process is thus modeled assuming steady-state conditions at different velocities. Considering the cement paste as a highly viscous liquid, the momentum balance equation writes:

$$\nabla P = \nabla \cdot (\eta \nabla \mathbf{v}) \,, \tag{2}$$

where P is the fluid pressure and η the apparent viscosity. For Non-Newtonian power-law fluids, the apparent viscosity η can be written as [14]:

$$\eta = K \cdot D_{eq}^{n-1} \cdot \mathbf{D}, \tag{3}$$

K and n being two material parameters, $\mathbf{D}$ the strain rate tensor and D_{eq} the equivalent strain rate tensor given by:

$$D_{eq} = \sqrt{\mathbf{D} : \mathbf{D}}. \tag{4}$$

The symbol " : " corresponds to the tensor product contracted twice. Since the LBB conditions are still unclear in a separated representation framework, the penalty method is used to solve the problem for the velocity field in the domain. This is initiated by expressing the conservation of mass as [15]:

$$\nabla \cdot \mathbf{v} = \lambda P, \tag{5}$$

with λ sufficiently small. Plugging equations (5) and (3) into the momentum balance equation (2), one can write:

$$\nabla \left(\nabla \cdot \mathbf{v} \right) = \lambda \cdot \nabla \cdot \left[\left(K \cdot D_{eq}^{n-1} \cdot \mathbf{D} \right) \nabla \mathbf{v} \right]. \tag{6}$$

Expression (6) represents the main equation to solve. The boundary conditions for the vane test represented in Figure 1 are expressed as:

$$\begin{cases} \mathbf{v} = \mathbf{0} \text{ at } R = 30 \text{ mm (non-slip condition)} \\ \mathbf{v} = \mathbf{0} \text{ at } z = 0 \text{ mm and } z = 120 \text{ mm} \\ \mathbf{v} = \mathbf{R} \times \omega \text{ at the contact with the vane (non-slip condition)} \end{cases} \tag{7}$$

where R is the radius measured from the dashed axis represented in Figure 1 and ω is the angular velocity of the vane.

For the vane test considered, a steady-state modeling approach entails that the problem be solved at each time step with the corresponding value of the angular velocity. The angular velocity is thus introduced as an extra coordinate of the problem, which yields the velocity field as a function of the spatial coordinates x, y, z and the angular velocity ω.

3 SOLVING THE NON LINEAR PROBLEM BY THE PGD

To solve the problem using the PGD, we start by expressing the weak form of equation (6). Denoting by $\mathbf{v}^*$ the test function, the weak form writes:

$$\int_\Omega (\nabla \cdot \mathbf{v}^*) \cdot (\nabla \cdot \mathbf{v}) d\Omega + \lambda \int_\Omega \nabla \left(\mathbf{D}^*\right)^T : \eta : \nabla \mathbf{D} d\Omega = 0. \tag{8}$$

The resolution of this four-dimensional problem – which ultimately yields $\mathbf{v}(x, y, z, \omega)$ – starts by a linearization process. The problem is thus solved first for $n = 1$, which is equivalent to considering a Newtonian fluid of apparent viscosity K. Solving the multidimensional problem requires introducing ω which only appears in the boundary conditions, as an extra coordinate. We thus act by means of a change of variables [8] and introduce the variable $\mathbf{F}$ satisfying the boundary conditions expressed in (7), i.e.:

$$\begin{cases} \mathbf{F} = \mathbf{0} \text{ at } R = 30 \text{ mm}, \\ \mathbf{F} = \mathbf{0} \text{ at } z = 0 \text{ mm and } z = 120 \text{ mm}, \\ \mathbf{F} = \mathbf{R} \times \omega \text{ at the contact with the vane, and} \\ \mathbf{F} = \mathbf{0} \text{ on the rest of the domain.} \end{cases} \tag{9}$$

We now define $\mathcal{V} = \mathbf{v} - \mathbf{F}$ and replace $\mathbf{v}$ by $\mathcal{V} + \mathbf{F}$ in equation (6). The problem can hence be resolved for $\mathcal{V}$ using homogeneous boundary conditions [8].

For the specific setting considered in this work, the spacial domain can be separated into a sum of $2D \times 1D$ domains. This said, the reduction in computational time that would result from such a decomposition is not significant because of the geometrical complexity. We thus choose to refrain from implementing any variable separation in 3D and hence to maintain the three-dimensional physical domain as represented in Figure 2. The meshed domain is shown in Figure 3.

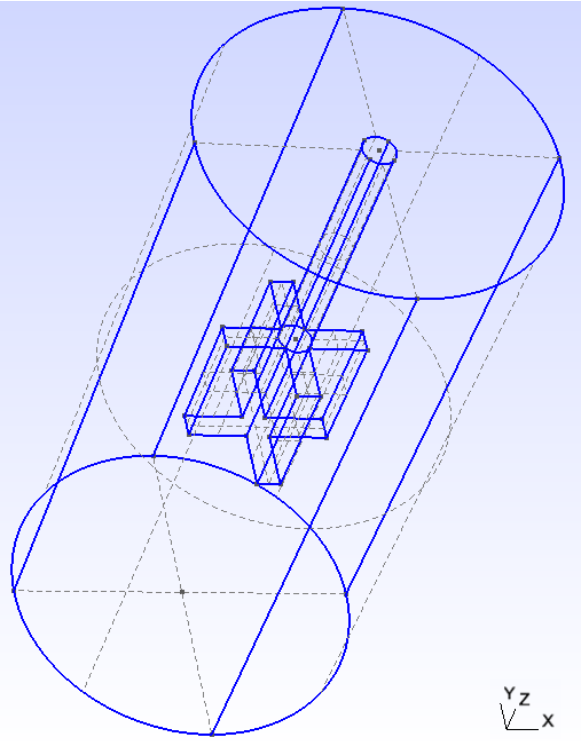

Figure 2: Illustration of the three-dimensional domain considered in the simulation.

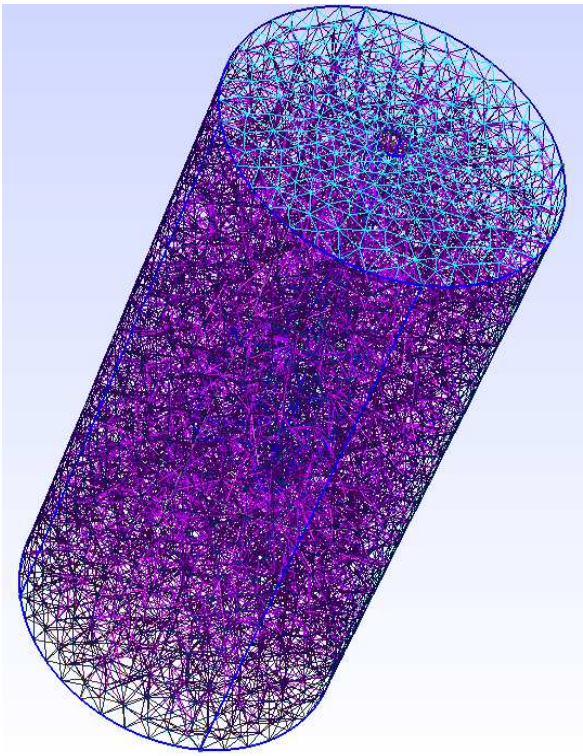

Figure 3: Mesh of the 3D considered domain obtained by using the Gmsh software.

The model's output corresponds to the velocity field $\mathbf{v}$ as a function of the spacial coordinates x, y, z and the angular velocity ω. This field is written in a separated form as:

$$\mathbf{v} = \begin{pmatrix} u(x,y,z,\omega) = \sum_{i=1}^{i=N} U_i(x,y,z) \cdot S_i(\omega) \\ v(x,y,z,\omega) = \sum_{i=1}^{i=N} V_i(x,y,z) \cdot S_i(\omega) \\ w(x,y,z,\omega) = \sum_{i=1}^{i=N} W_i(x,y,z) \cdot S_i(\omega) \end{pmatrix} \tag{10}$$

where u, v and w are the three components of the velocity vector along x, y and z respectively.

A fixed point iterative algorithm is used to solve the problem for Non-Newtonian fluids characterized by $n \neq 1$. The velocity profile obtained from the Newtonian solution is used as a first guess. At each iteration of the fixed point algorithm, a four-dimensional problem is resolved using the PGD. To this aim, all operators should be written in a separated form, including the operator multiplied by the viscosity η. Thus, at each iteration, the four-dimensional viscosity field $\eta(x,y,z,\omega)$ is determined using equation (3); it is then written in a separated form by means of a singular value decomposition (SVD). A new velocity field is finally determined from the separated viscosity result. The iterative process is repeated until the convergence of the viscosity η.

The material parameter K can be introduced as an extra coordinate of the problem at the expense of using a high order singular value decomposition (HOSVD) to write the viscosity in a separated form [16]. The HOSVD generates however approximation errors when writing the viscosity in a separated form and may lead to a dramatic reduction of the PGD's efficiency. The authors therefore prefer to use the PGD to solve $\mathbf{v}(x,y,z,\omega)$ and combine the PGD to a POD during the identification process to keep the problem as simple and accurate as possible.

4 RESULTS AND DISCUSSION

A typical example considering $K = 300$ Pa.s and $\omega = 0.5$ rad/s is retained. For this example, the nonlinear problem corresponding to the weak form in equation (8) is resolved with $n = 0.7$, 0.8, 0.9 and 1 respectively. A horizontal section at mid-height of the vane showing the magnitude superimposed to a quiver plot of the velocity field is provided in Figure 4 for each of these four cases.

Figure 4 reveals striking differences in the velocity fields between the cases corresponding to different values of n. In particular, a shear-thinning behavior can be clearly observed by comparing the cases $n = 0.7$ and $n = 1$, for example. This is for instance revealed by the sharp drop in the magnitude of the velocity field as one moves away from the tips of the blades in the case corresponding to $n = 0.7$ as opposed to the more homogeneous and gradual decrease of the same quantity between the tip of the blades and the outer cylinder

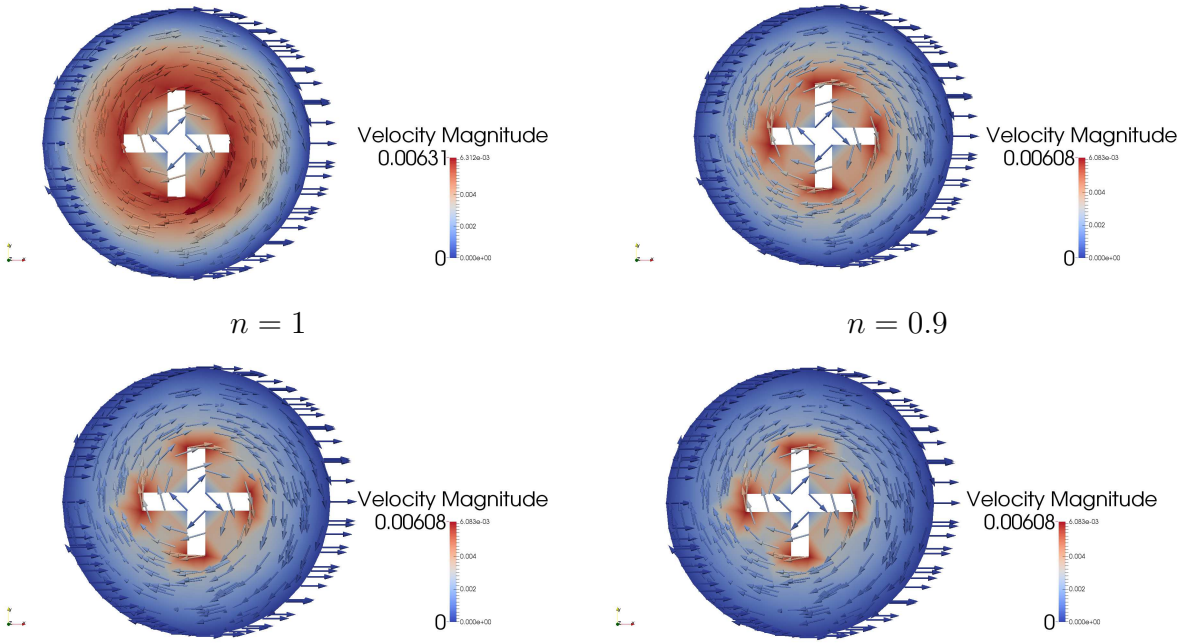

$n = 1$ $n = 0.9$

$n = 0.8$ $n = 0.7$

Figure 4: Typical magnitude and quiver plot of the velocity field; $n = 0.7$, 0.8, 0.9 and 1.

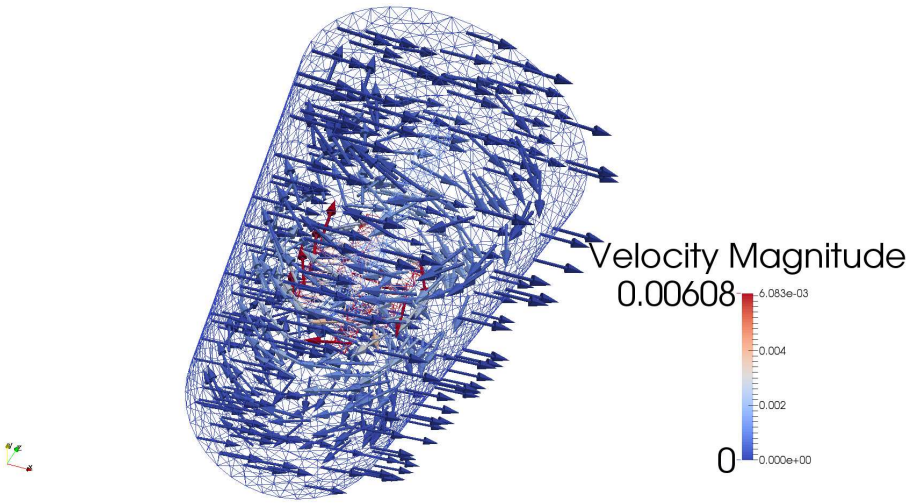

Figure 5: Typical 3D magnitude and quiver plot of the velocity field in the physical domain for $n = 0.7$.

when $n = 1$. A typical three-dimensional magnitude and quiver plot of the velocity field inside of the entire physical domain is also illustrated in Figure 5 at at $\omega = 0.5$ rad/s for $n = 0.7$.

One may also wish to determine the value of the torque applied to the vane – a quantity that is critical to the identification of material parameters from experimental results. To this aim, we distinguish in this work two origins of this torque: (i) the normal pressure field acting on the lateral surfaces of the blades of the vane and (ii) the shear stresses acting on the tips of the blades and on the vane's shaft. The contribution of the shear stresses acting radially on the lateral faces of the blades is neglected due to the their small eccentricity.

The normal pressure on the blades can be determined from equation (5), and thus the corresponding torque T_P expressed as:

$$T_P = \int_{A_1^*} P\mathbf{r} \times d\mathbf{A} - \int_{A_2^*} P\mathbf{r} \times d\mathbf{A}, \tag{11}$$

where A_1^* is the area of the vane surfaces upstream of the fluid flow and A_2^* downstream, $\mathbf{r}$ the radial distance from the axis of the vane to the point of application of the pressure and $d\mathbf{A}$ a differential area at this point. Figure 6 illustrates a typical variation of T_P for $n = 0.7$. The influence of n on the the part T_P of the torque that is due to the normal pressure acting on the lateral surfaces of the blades appears to be marginal.

The second component of the torque T_η that is due to the shear stresses is illustrated

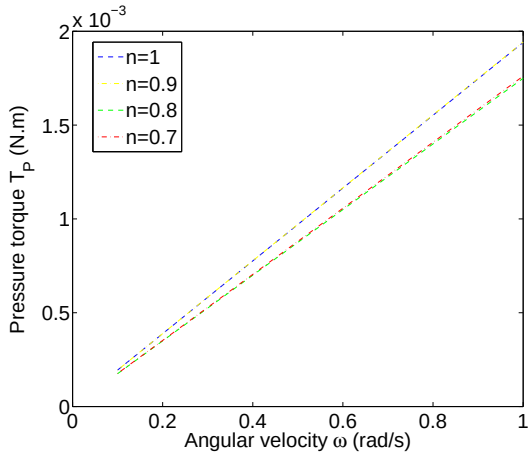

Figure 6: Torque T_p generated by the normal pressure on the blades for $n = 0.7$, 0.8, 0.9 and 1 as a function of ω.

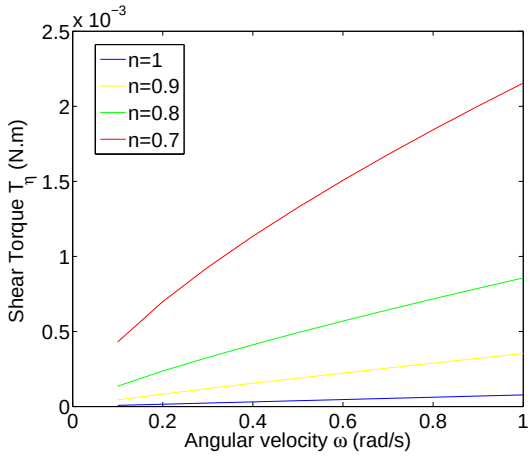

Figure 7: Torque T_η generated by the shear stresses acting on the tips of the blades for $n = 0.7$, 0.8, 0.9 and 1, as a function of ω.

in Figure 7. This component is defined by:

$$T_\eta = \int_{A^\dagger} \eta \cdot \mathbf{r} \times \nabla \mathbf{v} \cdot d\mathbf{A}, \tag{12}$$

where $A^\dagger$ corresponds to the area of the tip of the blades and of the upper circular shaft connecting the blades to the actuator. The dependence of T_η on n and ω appears to be strongly nonlinear. A linear variation of T_η as a function of ω can also be noted for $n = 1$.

In future work, the model's outputs shall be compared to experimental results to identify cement paste material properties K and n.

5 CONCLUSION

A novel approach to the modeling of the vane test on cement pastes using Non-Newtonian power-law fluids is proposed in this work, with the final objective of identifying material properties of the pastes. The PGD is used to simulate the fluid flow in the vane test while introducing the mixing velocity as an extra coordinate. The nonlinear four-dimensional problem is addressed using the PGD by means of a first linearization process using a fixed-point iterative algorithm. The full resolution process – involving 100 nodes in ω and 16050 finite elements discretizing the 3D spatial domain – typically takes a few minutes only, on a normal portable PC.

The proposed model replicates successfully the nonlinear behavior of the torque as a function of the angular velocity. Such behavior is typically observed experimentally when running vane tests on cement pastes.

REFERENCES

[1] G. Ovarlez and N. Roussel. A physical model for the prediction of lateral stress exerted by self-compacting concrete on formwork. *Materials and structures*, 39:269Ű279, 2006.

[2] W. Wang, D. De Kee, and D. Khismatullin. Numerical simulation of power law and yield stress fluid flows in double concentric cylinder with slotted rotor and vane geometries. *Journal of Non-Newtonian Fluid Mechanics*, 166:734–744, 2011.

[3] Chady Ghnatios, Francisco Chinesta, and Christophe Binetruy. 3d modeling of squeeze flows occuring in composite laminates. *International Journal of material forming*, 8(1):73–83, March 2015.

[4] S. Aghighi, A. Ammar, C. Metivier, M. Normandin, and F. Chinesta. Non incremental transient solution of the rayleigh-benard convection model using the pgd. *Journal of Non Newtonian Fluid Mechanics*, 200:65–78, 2013.

[5] Chady Ghnatios, Francoise Masson, Antonio Huerta, Elias Cueto, and Francisco Chinesta. Proper generalized decomposition based dynamic data-driven of thermal processes. *Computer Methods in Applied Mechanics and Engineering*, 213-216:29–41, 2012.

[6] Howard Anthony Barnes and Quoc Dzuy Nguyen. Rotating vane rheometry - a review. *Journal of Non Newtonian Fluid Mechanics*, 98(1):1–14, March 2001.

[7] Petra V. Liddel and David V. Boger. Yield stress measurment with the vane. *Journal of Non-Newtonian Fluid Mechanics*, 63(2-3):235–261, April 1996.

[8] Chady Ghnatios, Francisco Chinesta, Elias Cueto, Adrien Leygue, Arnaud Poitou, Piotr Breitkopf, and Pierre Villon. Methodological approach to efficient modeling and optimization of thermal processes taking place in a die: Application to pultrusion. *Composite Part A : Applied Science and Manufacturing*, 42:1169–1178, May 2011.

[9] Chady Ghnatios. *Modélisation avancée des procédés thermiques rencontrés lors de la mise en forme des composites*. PhD thesis, Ecole Centrale Nantes, October 2012.

[10] Francisco Chinesta, Amine Ammar, and Elias Cueto. Recent advances in the use of the proper generalized decomposition for solving multidimensional models. *Archives of Computational Methods in Engineering*, 17(4):327–350, 2010.

[11] Francisco Chinesta, Amine Ammar, and Elias Cueto. Recent advances and new challenges in the use of the proper generalized decomposition for solving multidimensional models. *Archives of Computational Methods in Engineering*, 17(4):327–350, December 2009.

[12] Etienne Pruliere, Julien Ferec, Francisco Chinesta, and Amine Ammar. An efficient reduced simulation of residual stresses in composite forming processes. *International Journal of Material Forming*, 3:1339–1350, 2010.

[13] Chady Ghnatios. Optimization of composite forming processes using non-linear thermal models and the proper generalized decomposition. In IEEE-xplore, editor, *Third International Conference on Advances in Computational Tools for Engineering Applications (ACTEA)*, 2016.

[14] Jean François Agassant, Pierre Avenas, Jean-Philippe Sergent, Bruno Vergnes, and Michel Vincent. *La mise en forme des matières plastiques*. Lavoisier, 1996.

[15] Jean Donea and Antonio Huerta. *Finite element method for flow problem*. Wiley, 2003.

[16] Tamara G. Kolda and Brett W. Bader. Tensor decompositions and applications. *Society for Industrial and Applied Mathematics*, 51(3):455–500, 2009.